Long-term pig manure application increases SOC through aggregate protection and Fe-C associations in a subtropical Red soil (Udic Ferralsols)

Hui Rong[a], Zhangliu Du[b], Weida Gao[a], Lixiao Ma[c], Xinhua Peng[d], Yuji Jiang[e], Demin Yan[f], Hu Zhou[a,]

[a] *Key Laboratory of Arable Land Conservation (North China), Ministry of Agriculture, College of Land Science and Technology, China Agricultural University, Beijing, China*

[b] *College of Resources and Environmental Sciences, China Agricultural University, Beijing 100193, China*

[c] *State Key Laboratory of Vegetation and Environmental Change, Institute of Botany, Chinses Academy of Sciences, Beijing 100093, China.*

[d] *Institute of Agricultural Resources and Regional Planning, Chinese Academy of Agricultural Sciences, Beijing 100081, China*

[e] *College of Resources and Environment, Fijian Agriculture and Forest University, Fuzhou, 350002, China.*

[f] *College of Criminal Science and Technology, Nanjing Police College, Nanjing 210023, China.*

Correspondence: Hu Zhou (zhouhu@cau.edu.cn)

Abstract

Manure is known to improve soil organic carbon (SOC) in Fe-rich red soils, but the underlying stabilization mechanisms remain poorly understood. A long-term field experiment was conducted with four treatments: no amendment (Control), low manure (LM, 150 kg N ha^{-1} yr^{-1}), high manure (HM, 600 kg N ha^{-1} yr^{-1}), and high manure with lime (HML, 600 kg N ha^{-1} yr^{-1} plus 3000 kg Ca $(OH)_2$ ha^{-1} $3yr^{-1}$). The quantity and quality of SOC were characterized by physical fractionation, ^{13}C NMR spectroscopy and thermogravimetry (TG) analysis from 0-20 cm depth. Manure application increased total SOC by 65.1%-126.7%, with the increase primarily occurring in the particulate organic matter (POM) fraction. Specifically, POM C increased substantially by 208%-592%, compared to a 32.0% -66.8% increase in MAOM C. POM C was stabilized through the process of hierarchical aggregation. Fresh manure inputs acted as binding nuclei, leading to an increase in macroaggregates (>0.25 mm) concurrently with a reduction in microaggregates (0.05–0.25 mm), physically isolating labile C from microbial decomposition. Concurrently, manure amendments triggered Fe-mediated chemical stabilization. The elevated pH (4.8 to 5.4-7.1) in the manure treatments enhanced non-crystalline Fe oxide (Fe_o) content by 25.4%, which positively correlated with MAOM C (R^2 = 0.56, P < 0.05). Despite chemical composition shift toward aliphaticity and

reduced aromaticity, thermally stable organic matters increased by 8%–12%, revealing the critical role of Fe_o in offsetting inherent molecular lability when aggregate protection was removed by destruction prior to TG analysis. Overall, this study proposes a dual SOC stabilization framework via physical and chemical Fe-carbon associations in a subtropical red soil.

Keywords: Particulate organic matter; Mineral-associated organic matter; Nuclear magnetic resonance; Thermogravimetry analysis

1. Introduction

Soil organic carbon (SOC), the largest carbon reservoir in the terrestrial ecosystems, plays critical roles in climate mitigation and soil multifunctionality (Amelung et al., 2020; Lal, 2004). Red soils (Udic Ferralsols, according to Chinese Soil Taxonomy) have low SOC content due to intense weathering and rapid mineralization in tropical and subtropical South China (Yan et al., 2013; Zhang et al., 2013). While manure has been widely used to enhance SOC in these soils (Bai et al., 2023; Nichitha et al., 2023; Zhang et al., 2023), the underlying mechanisms governing its stabilization remain elusive. Currently, the discrepancies existed regarding the manure-induced SOC accrual through chemical recalcitrance, physical protection (by aggregation processes), or organo-mineral interactions—given the Fe-enrich red soils and their pH-dependent reactivity (Kleber et al., 2021; Six et al., 2002; Song et al., 2022). Considering, the red soils covering 22% of China's cropland and low inherent SOC levels, it is essential to unveil Fe-C interactions that regulate SOC stabilization through organic amendments.

Existing studies showed some conflicting evidences on SOC stabilization pathways. For instance, Mustafa et al. (2021) reported increased aromatic C (chemically recalcitrant) with manure application, whereas Yan et al. (2013) observed preferential accumulation of labile O-alkyl C. This paradox highlighted uncertainties on how manure inputs altered SOC composition. It is reported that Fe oxides contributed to SOC stabilization in red soils (Zhang et al., 2013). These reactive Fe phases can form stable covalent bonds between their surface hydroxyls and organic functional groups, protecting SOC from microbial decomposition (Ruiz et al., 2024). In comparison with crystalline Fe oxides (Fe_d), non-crystalline Fe oxides (Fe_o) exhibit organic matter adsorption capacity primarily attributed to their larger specific surface area (Zhang et al., 2013). Previous

studies have demonstrated that long-term application of organic fertilizers—including manure, compost, and straw—significantly increased amorphous iron oxides (Fe_o) in agricultural soils (Chen et al., 2022; Huang et al., 2018; Wang et al., 2019). These studies further revealed that redox cycling promoted the reductive dissolution of crystalline iron (Fe_d), followed by its reprecipitation as amorphous Fe_o during oxidative periods. On the other hand, soil pH was identified as a key factor dynamically influencing the Fe_d/Fe_o ratio (Liu et al., 2020; Wang et al., 2023). Although organic amendments are known to elevate pH in acidic red soils, the specific effect of soil pH modulating the formation and stabilization of Fe_o remains unclear. Additionally, previous studies widely isolated chemical recalcitrance, aggregation protection, or organo-mineral interactions separately, largely neglecting the integrative assessments including these pathways. To address this knowledge gap, an integrative approach combining physical fractionation, molecular characterization, and thermal stability analysis is essential for elucidating the coupled effects of manure on SOC quantity and quality.

Physically separating soil organic matter (SOM) into mineral-associated organic matter (MAOM) and particulate organic matter (POM) fractions could help to predict SOC dynamics, and clarify SOC stabilization mechanisms. The POM associated SOC (defined as POM C) physically protected in the macroaggregates, while MAOM associated SOC (defined as MAOM-C) chemically protected via organo-mineral bonding (Chenu et al., 2019; Lavallee et al., 2019; Poeplau et al., 2018). Although physical fractionation could effectively isolate operationally defined these SOC pools (Poeplau et al., 2018), it failed to reveal the chemical heterogeneity of SOC (Cotrufo et al., 2019; Lavallee et al., 2019). Thus, solid-state ^{13}C NMR spectroscopy could address this gap by quantifying SOC functional groups (e.g. alkyl, O-alkyl, aromatic C), after completely disrupting organo-mineral interaction by HF pretreatment (Kögel-Knabner, 1997). Additionally, the thermogravimetry (TG) could rapidly assess the thermal stability of SOC without requiring pretreatment (Gao et al., 2015). On the other hand, some advanced techniques such as nano-scale secondary ion mass spectrometry (NanoSIMS) and high-resolution mass spectrometry could identify the spatial visualization of organo-mineral associations and molecular characterization, these approaches heavily required complex instrumentation and are not cost-effective for the comparative analysis of multiple samples. Therefore, combined NMR with TG approaches to efficiently evaluate the chemical composition

and thermal stability of SOC in response to manure management.

The specific objectives of this study were: 1) to evaluate the changes of Fe oxides and its effect on MAOM formation; 2) to explore how soil aggregation affected POM formation; 3) to evaluate the effect of manure application on SOC composition and stability. We hypothesized that: 1) Manure application could enhance MAOM C formation by increasing non-crystalline Fe oxides (Fe_o), induced by elevated pH; 2) Manure application would strengthen the physical protection due to the improved soil aggregation, which triggered labile SOC protection; 3) The application of pig manure would boost the recalcitrance of SOC, thus the thermal stability.

2. Materials and methods

2.1. Site description and experimental design

The long-term field experiment is located at Yingtan National Agroecosystem Field Experiment Station of the Chinese Academy of Sciences (28°15′20″N, 116°55′30″E) in Jiangxi Province, China. The site has a typically subtropical humid monsoon climate with a mean annual temperature of 17.6℃ and precipitation of 1795 mm (Jiang et al., 2018). The soil is derived from Quaternary red clay, and is classified as Udic Ferralsols according to Chinese Soil Taxonomy. The soil contains 36.3% clay, 45.2% silt and 21.2% sand.

The field experiment was initiated in April, 2002. The soils used in this experiment were transported from adjacent forestland and repacked (to a depth of 2 m) for all the plots. This design ensures a uniform initial soil condition and eliminates the influence of prior land use history. Four treatments were compared: (1) no manure amendment (Control), (2) low pig manure with 150 kg N ha^{-1} a^{-1} (LM), (3) high pig manure with 600 kg N ha^{-1} a^{-1} (HM), and (4) high pig manure with 600 kg N ha^{-1} a^{-1} and lime (HML). The four treatments received solely pig manure as the nitrogen source, with no synthetic fertilizers applied. The pig manure, collected from nearby pig farms, contained an average total carbon of 386.5 g kg^{-1}, total nitrogen of 36.2 g kg^{-1} and total phosphorus of 21.6 g kg^{-1} on a dry matter basis. The annual amount of pig manure applied to each treatment was calculated based on its nitrogen content. Since all aboveground residues (stalks and leaves) and manually recoverable roots were completely removed from the field after harvest, the total carbon inputs to the soil were derived mainly from pig manure**.** This resulted in average annual carbon inputs of

around 1.6 and 6.4 Mg C ha^{-1} for the LM and HM treatments, respectively (see Supplementary Material for calculation details). The field experiment was set up following a completely randomized design, with each treatment has three replicate plots. Lime was applied at 3 000 kg $Ca(OH)_2$ ha^{-1} $(3a)^{-1}$ for the HML treatment. The field was planted with corn (*Zea mays L.*) monoculture annually from April to July. The pig manure was applied annually each April onto the soil surface (0-10 cm depth) and subsequently incorporated into the topsoil through plowing and harrowing. All the management measures, including sowing, harvesting and weeding, were manually operated.

2.2 Sampling

Sampling was conducted in July 2019, after the harvest of corn. Triplicate topsoil samples (0-20 cm) were randomly collected with a shovel from each plot and composited together to form one bulk sample. The soil samples were air-dried at room temperature and were gently crushed with a rubber mallet to pass through an 8-mm sieve, preserving aggregates >8mm for further analysis. Visible plant residues, roots and stones were removed (Soil Survey Staff, 2011). No visible manure residues were observed.

2.3 Soil properties measurements

SOC and Total nitrogen (TN) were determined by an elemental analyzer (Vario MACRO, Elementar, Germany). Soil pH was measured using a glass electrode (PHS-3D, SANXIN, China) with soil: deionized water ratio of 1: 2.5. Crystalline (Fe_d) and non-crystalline Fe oxides (Fe_o) were extracted by DCB (Dithionite-citrate-bicarbonate) and oxalate, respectively (Yan et al., 2013), and then were determined by graphite furnace atomic absorption spectrometry (GFAAS) (PinAAcle 900T, PerkinElmer, America). Water stability of aggregates was tested using the fast-wetting method following Le Bissonnais (1996). Aggregate stability was expressed as mean weight diameter (MWD). Detailed experimental processes and calculation can be found in Zhou et al. (2019).

2.4. Physical fractionation

Soil was fractionated into MAOM (<53 μm) and POM (>53 μm) fraction following Cambardella and Elliott (1992) and Cotrofu et al. (2019). Briefly, 10 g sieved samples (<2 mm) were dispersed in dilute sodium hexametaphosphate ($(NaPO_3)_6$, 0.5%) at a soil: solution ratio of 1:4 by shaking for 18 h (25°C, 180 r min^{-1}). This procedure primarily disrupts macroaggregates (>250 μm), but remaining that stable microaggregates (<53 μm). After dispersing, soil slurry was passed through a

53 μm sieve and rinsed several times with deionized water. The fraction passing through the sieve was collected as MAOM fraction, and that remaining on the sieve was collected as POM fraction. Both fractions were centrifuged and the solution was decanted, and then the remaining material was oven-dried to constant weights at 60℃. SOC concentration of each fraction was measured using the wet oxidation method. Dried mass proportions of each fraction (g fraction g^{-1} soil) were calculated as follows:

$$f_M = m_M / m_{bulk} \quad (1)$$

$$f_P = m_p / m_{bulk} \quad (2)$$

where f_M and f_P were the dried mass proportions of MAOM and POM fraction (g fraction g^{-1} bulk soil), respectively; m_M and m_P (g)were the dried masses of MAOM and POM fractions; m_{bulk} (g) was the dried mass of bulk soil.

SOC in the MAOM and POM fractions were called as MAOM C and POM C, respectively in this paper. MAOM C and POM C were calculated by multiplying the dried mass proportions of each fraction (g fraction g^{-1} soil) by the respective SOC concentrations (g C kg^{-1} fraction) as follows (Garten and Wullschleger, 2000; Lian et al., 2015):

$$\text{MAOM C} = f_M \times \text{SOC}_M \quad (3)$$

$$\text{POM C} = f_P \times \text{SOC}_P \quad (4)$$

where f_M and f_P were calculated by Equation (1) and Equation (2); SOC_M and SOC_P were the SOC concentrations in the MAOM and POM fraction (g C kg^{-1} fraction), respectively.

The contributions of MAOM C and POM C to total SOC (%) was calculated as:

$$\text{Contribution of MAOM C (\%)} = \text{MAOM C} / \text{Total SOC} \times 100 \quad (5)$$

$$\text{Contribution of POM C (\%)} = \text{POM C} / \text{Total SOC} \times 100 \quad (6)$$

where MAOM C and POM C were derived from Equations (3) and (4), respectively; total SOC was the content of SOC in the bulk soil.

2.5. SOC chemical composition and chemical stability

SOC chemical composition was analyzed with a solid-state cross-polarization magic angle spinning (CPMAS) ^{13}C nuclear magnetic resonance (NMR) spectroscopy. Prior to NMR analysis, <2 mm air-dried soils were pretreated with hydrofluoric acid (HF) to remove paramagnetic Fe^{3+} (iron oxides) following Gao et al. (2021). While HF pretreatment can dissolve short-range-order

minerals and potentially disrupt certain organo-mineral associations, it is an essential step to improve the signal-to-noise ratio and spectral resolution required for the reliable quantification of carbon functional groups. Firstly, 20 g soil was mixed with 100 mL 10% (w/w) HF solution in a polyethylene bottle and then shaken for 0.5 h per day for three days. Afterwards, the supernatant liquid was discarded and another 100 mL 10% HF solution was added again. The above procedures were repeated for 15 times. The residue was rinsed 10 times with deionized water until the pH was close to neutral. The remaining soil was freeze-dried and then ground in an agate mortar to pass through a 100-mesh sieve (0.149 mm) for further analysis. This fine grinding ensured homogeneous packing in the NMR rotor, minimizing signal heterogeneity (Simpson & Simpson, 2012).

Carbon functional groups were determined with the Bruker Ascend 500 MHz NMR spectrometer (Bruker BioSpin, Rheinstetten, Germany). Dry powdered samples were placed in a 4-mm sample rotor operating at a ^{13}C resonance frequency of 125.8 MHz. The NMR spectrometer run at a spinning rate of 5kHz, and 10500 scans were collected for each sample. The spectra were collected over an acquisition time of 12 ms and a recycle delay of 0.8 s. All obtained spectra were processed with phase and baseline corrections. To allow for a direct comparison of the relative distribution of carbon functional groups, the total spectral intensity of each spectrum was normalized to that of the control soil sample. The normalized spectra were then integrated across and we assigned the obtained spectra to four different carbon functional groups, i.e., alkyl C (0-45 ppm), O-alkyl C (45-110 ppm), aromatic C (110-160 ppm) and carbonyl C (160-220 ppm) according to Kögel-Kanbner (1997). The relative concentrations of the different functional groups were calculated as the percentage of their peak areas to the total aeras using MestReNova 14.0 software (Mestrelab Research, 2019, Spain). Indices used to evaluate SOC recalcitrance include: alkyl C/O-alkyl C, aromaticity, aromatic C/O-alkyl C, aliphatic C/aromatic C and aliphaticity (Baldock et al., 1997; Du et al., 2017). Aromaticity = aromatic C / (alkyl C + O-alkyl C + aromatic C); Aliphatic C = alkyl C + O-alkyl C; Aliphaticity = (alkyl C + O-alkyl C) / (alkyl C + O-alkyl C + aromatic C). The alkyl C/O-alkyl C ratio reflects the degree of microbial transformation, with higher values indicating advanced decomposition and accumulation of recalcitrant alkyl compounds (Baldock et al., 1997). The aromatic C/O-alkyl C ration aligns with the alkyl C/O-alkyl C ration in reflecting the degree of SOC decomposition, whereas the aliphatic C/aromatic C ratio presents a contrary perspective to them. Aromaticity is a

chemical concept denoting the resistance to microbial degradation (Kögel-Knabner, 1997). Aliphaticity is used to quantify the proportion of labile aliphatic components relative to stable aromatic moieties.

2.6. Thermogravimetry analysis

TG analysis was performed using a Netzsch TG 209F1 (Netzsch-Gerätebau GmbH, Selb, Germany). Air-dried soil samples were first sieved through a 2-mm mesh, and then ground in a ball mill to pass through a 50 μm sieve. The grounded soil samples (5 ~ 10 mg) were placed in an Al_2O_3 crucible covered with an aluminum lid and were oxidized in an atmosphere of 20 mL min^{-1} of synthetic air (20% O_2 and 80% N_2) and 20 mL min^{-1} of N_2 as a protective gas. The temperature program included a heating rate of 10°C min^{-1} from 40°C up to 800°C. The sample mass percentage relative to the initial mass as a function of temperature was recorded simultaneously, and its first derivative (DTG) was calculated to represent the mass loss rate.

Three processes were detected in the temperature range of 40°C to 800°C: hygroscopic moisture evaporation, SOM decomposition and carbonate breaking down (Gao et al., 2015; Siewert, 2004). Based on the observed DTG curve, the weight loss between 180°C and 530°C, representing the temperature range during which SOM was decomposed, was defined as the total mass of SOM (Exo_{tot}). The mass loss between 180°C and 380°C was a consequence of thermally labile SOM oxidation (Exo_1) and that between 380°C and 530°C was caused by the combustion of more stable organic matter (Exo_2) (Gao et al., 2015; Volkov et al., 2020). We used two parameters, the ratio of Exo_1 and Exo_{tot} (Exo_1/ Exo_{tot}) and the temperature at which half of the SOM was decomposed (TG-T_{50}), to characterize the thermal stability of SOM. Higher Exo_1/ Exo_{tot} and lower TG-T_{50} values indicate that the sample has more thermally labile or unstable SOM (Gao et al., 2015; Siewert, 2004).

2.7. Statistical analysis

Statistical analyses were carried out with R Studio software (R Development Core Team, version 4.1.2). One-way analysis of variance (ANOVA) was conducted to assess the effect of amendments on soil physico-chemical properties, SOC physical fractions, chemical composition and thermal indices. The independence of samples, normality of residuals and homogeneity of variances were checked by Chisq, Shapiro-Wilk and Bartlett test, respectively. Fisher's least significant difference (LSD) method was used for the multiple comparisons of means with a 0.05 significance level. Linear

regression analysis was conducted to investigate the correlations between SOC and iron oxides, soil aggregation. Principal component analysis (PCA) was performed to evaluate the relationship between the quantity and quality of SOC and factors related to chemical protection and physical protection. Pearson correlation analyses were performed to explore the relationships between chemical composition and thermal indices.

3. Results

3.1. Long-term pig manure application increased SOC, TN, pH, non-crystalline (Fe_o) and improved soil aggregation

Long-term manure amendment altered the soil physico-chemical properties (Table 1). Relative to the Control, the SOC concentration was 64.9%, 116.2% and 126.6% higher in the LM, HM and HML treatments, respectively ($P < 0.05$), and TN concentration was 48.0%-108.2% higher ($P < 0.05$). The pH values were 0.62-2.28 units higher than those in the Control ($P < 0.05$). Application of pig manure had no significant effect on crystalline iron oxides (Fe_d) content ($P > 0.05$), but the HM and HML treatments showed significantly greater non-crystalline iron oxides (Fe_o), with an increase of 25.4% relative to the Control ($P < 0.05$). Compared to the Control, the HM and HML treatments had significantly higher macroaggregates (>0.25 mm) content by 15.8% and 16.8%, respectively, and greater mean weight diameter (MWD) by 24.3% and 35.0% ($P < 0.05$). In contrast, microaggregates (0.05-0.25 mm) was lower under the HM and HML treatments, with reduction of 30.4% and 36.4%, respectively ($P < 0.05$).

3.2. Long-term pig manure application affected SOM physical fractions: MAOM and POM

The distribution of MAOM and POM fractions was significantly influenced by manure and lime amendments ($P < 0.05$, Table 2). Across all treatments, MAOM dominated the soil mass proportion (72.5%–75.1%), whereas the proportion of POM was progressively higher, ranging from 16.6% in the Control to 19.3%–19.4% under the HM and HML treatments.

Manure application improved SOC concentration in both fractions. SOC in the MAOM fraction was 32.0%-66.8% greater, and that in the POM fraction was 208%-592% greater relative to the Control. The contribution of MAOM to total SOC was lower in the HM and HML treatments (65.5%-65.8%) than in the Control (82.4%), while the contribution of POM was nearly threefold higher (increasing from 8.8% to 23.7%–26.0%). Lime addition (HML vs. HM) did not significantly

alter mass proportions but further enhanced POM C concentration (+15.4%) and its contribution to total SOC (+9.7%).

3.3. Effect of long-term pig manure application on SOC chemical composition and recalcitrance

The solid-state ^{13}C NMR spectra showed different signal patterns for the different treatments (Fig. 1) and quantified the ratios of the different SOC functional groups shown in Table 3. Relative to the Control, the HM and HML treatments had a significantly higher proportion of alkyl C by 4.6%-4.9% ($P < 0.05$), while the LM treatment showed no significant difference ($P > 0.05$). The proportion of O-alkyl C was also significantly higher under the LM, HM and HML treatments, with increases of 5.5%, 2.6% and 2.2%, respectively ($P < 0.05$). In contrast, the proportions of aromatic C and carbonyl C were lower in the manure-amended treatments, with reduction of 12.4%-13.2% and 0.9%-8.7%, respectively ($P < 0.05$).

Relative to the Control, the alkyl C/O-alkyl C ratio was significantly lower under the LM treatment ($P < 0.05$), whereas the HM and HML treatments had no significant effect on the ratio ($P > 0.05$, Table3). The aromaticity was decreased by 14.4%, 12.9% and 13.2% under LM, HM and HML treatments, respectively ($P < 0.05$, Table3). Similarly, the aromatic C/O-alkyl C ratio was 14.7%-17.7% lower in the manured treatment ($P < 0.05$, Table3). Conversely, both the aliphatic C/aromatic C ratio and aliphaticity were higher in the manured treatments, with elevations of 18.1%-20.7% and 2.44%-3.66%, respectively ($P < 0.05$, Table3).

3.4. The effect of long-term pig manure application on SOC thermal stability

The shapes of TG and its first derivatives (DTG) curves showed distinct weight losses rate as temperature increased to above 100℃, in the order of HM>HML>LM>Control (Fig. 2). Relative to the Control treatment, pig manure application significantly increased the total mass losses in the range of 180℃ to 530℃ (Exo_{tot}) by 11.1%- 17.4% ($P < 0.05$, Table 4), and significantly increased the mass losses during 180-380℃ (Exo_1) and 380-530℃ (Exo_2) by 14.6%-26.5% and 7.8%-13.7%, respectively ($P < 0.05$, Table 4). The ratio of Exo_1/Exo_{tot} was significantly elevated in the LM and HM treatments ($P < 0.05$), whereas the HM treatment showed no significant effect relative to the Control ($P > 0.05$, Table 4). HM and HML treatments significantly decreased TG-T_{50} by 10.7-12.0 ℃ ($P < 0.05$), while LM treatments showed no significant difference compared to Control ($P > 0.05$, Table 4).

3.5. *Relationships between SOC and factors related to the mineral protection and physical protection of SOC*

Fig. 3 showed correlations between SOC and possible variables associated with the chemical protection and physical protection of SOC. SOC in the bulk soil was significantly positively correlated with MAOM C (R^2=0.97, Fig. 3A). MAOM C showed no relationship with Fe_d (R^2=0.04, Fig. 3B), it was positively correlated with Fe_o (R^2=0.56, Fig. 3C). A weaker correlation was observed between MAOM C and the content of clay and silt (R^2 = 0.34, P = 0.46, Fig. 3D). Notably, Fe_o concentration was significantly and positively correlated with pH (R^2=0.59, P<0.01; Fig. 4A). Conversely, the concentration of Fe_d was not correlated with pH (P>0.05; Fig. 4B).

SOC in the bulk soil was significantly positively correlated with POM C (R^2=0.95, Fig. 3E). POM C was significantly associated with soil aggregation, evidenced by the positive correlation with macroaggregates (>0.25 mm) (R^2=0.78, Fig. 3F) and MWD (R^2=0.67, Fig. 3H), while negative correlation with microaggregates (<0.25 mm) (R^2=-0.71, Fig. 3G).

A PCA plot diagram (Fig. 5) revealed distinct associations between SOC quantity/quality and stabilization mechanisms. SOC vector aligned positively with POM C, macroaggregates and MWD, but inversely with microaggregates. Chemically, SOC covaried with MAOM C and Fe_o, yet formed an obtuse angle (>90°) with Fe_d. TG-T_{50} negatively associated with the proportion of O-alkyl C and aliphaticity (angles > 90°), but positively linked to aromatic C and aromaticity (angles < 90°).

4. Discussion

4.1. POM C and physical protection

Long-term pig manure application caused an increase of SOC in the bulk soil relative to the Control, and the increase was mainly derived from continuous manure inputs (Gong et al., 2009). Although maize rhizodeposition (including root exudates and sloughed-off cells) (typically <10% of net primary productivity; Pausch and Kuzyakov, 2018) contributes to SOC during the growing season, its annual carbon inputs are only 0.2-0.5 Mg C ha^{-1} yr^{-1} (Dennis et al., 2010). This plant-derived C input is much lower than that from manure, which ranged from 1.6 to 6.4 Mg C ha^{-1} yr^{-1} in the LM and HM treatments, respectively. The rigorous removal of all harvest residues (stalks and recoverable roots) minimized aboveground and root biomass as a source of soil carbon deposition. It should be noted that some residual plant-derived materials (e.g., fine root fragments and exudates)

have contributed marginally to the SOC pool. Given the relatively small quantity of plant-derived carbon inputs, the changes in SOC observed in this study are primarily attributable to the application of pig manure. Following microbial decomposition and transformation, the applied manure-C was progressively partitioned into distinct SOC pools.

Manure-derived carbon was preferentially allocated to the POM fraction rather than the MAOM fraction. The contribution of POM C to SOC in the manure-amended treatment was nearly threefold as that in the Control (8.8% to 26.0%), while the proportion of MAOM C decreased significantly from 82.4% in the Control to 65.4%–71.0% in the manure application treatments (Table 2). The result was in line with Lan et al. (2022) and Li et al. (2018), who reported that increased manure substitution improved the POM C/MAOM C ratio, indicating manure was beneficial to the formation of POM C. These results implied carbon inputs are preferentially stabilized as POM rather than MAOM. This finding is supported by biomarker evidence showing a great contribution of plant-derived carbon to the POM fraction (Zou et al., 2023). Consistent with this, a ^{13}C isotopic tracing study revealed that 70%-87% of residue-derived SOC was accumulated in the POM fraction at two experimental sites (Mitchell et al.,2021). The mechanism behind this preferential sequestration is the physical occlusion of fresh organic material within macroaggregates, which provides initial protection against rapid microbial decomposition. Therefore, POM C can be a good indicator of SOC dynamics under field management (Álvaro-Fuentes et al., 2021; Wu et al., 2023)..

While POM C is inherently labile and susceptible to decomposition, it can be physically protected from rapid decay through occlusion within stable soil aggregates. According to the classical hierarchical aggregation model (Six et al., 2000), organic carbon acts as a primary binding agent for microaggregates (<0.25mm) to form macroaggregates (>0.25mm), with POM serving as both a structural nucleus and a transient carbon reservoir (Six et al., 2000). In this study, macroaggregates were significantly increased, and free microaggregates were significantly decreased after pig manure application (Table 1). These results implied that manure-derived carbon acted as binding agent, promoting the formation of macroaggregates from free microaggregates. This process provides physical protection for SOC, particularly that in the POM fraction, within the newly formed aggregates, particularly in the POM fraction (Peng et al., 2023). The observed positive correlation between POM C and both macroaggregates and aggregate MWD (Fig.3; Fig.4) further

suggested the critical role of soil aggregation. However, the physical mechanisms by which POM facilitates this process (e.g., microbial mediation, hydrophobic interactions, or polysaccharide bridging) require further investigation. Experimental approaches such as isotopic labelling combined with micro-scale imaging (e.g., electron microscopy or X-ray computed tomography) can visualize the spatial distribution of POM within aggregates and quantify its role in aggregate formation. Future study should pay attention to these new technologies.

4.2. MAOM C and chemical protection

MAOM retained higher SOC concentrations (4.18-7.09 g C kg^{-1} bulk soil) than the POM fraction did, irrespective of treatments, though its contribution to total SOC decreased after manure application (Table 2). MAOM C remained the dominant SOC reservoir, consistently comprising over 65% of the total SOC across all treatments (Table 2). This underscores that organo-mineral complexation, rather than physical protection within aggregates, is the primary stabilization pathway in these red soils, even under significant organic input. MAOM C exhibited significantly longer mean residence time (MRT) compared to POM C, with reported turnover periods of 26-40 years versus 2.4-4.3 years, respectively (Benbi et al., 2014; Garten and Wullschleger, 2000). This fundamental difference originates from the unique stabilization mechanism of MAOM C through persistent organo-mineral associations (Lavallee et al., 2019). While clay minerals are widely recognized as key MAOM stabilizers (Hemingway et al., 2019; Liang et al., 2017), our study reveals a distinct iron oxide-dominated mechanism in these Fe-rich red soils. The strong correlation between MAOM C and non-crystalline Fe oxides (Fe_o, R^2=0.56; Figs. 3C, 4) highlighted the pivotal role of Fe_o on SOC stabilization in this red soil. This iron-mediated stabilization likely stems from the exceptionally high specific surface area of Fe_o (~800 m^2 g^{-1} in ferrihydrite; Kleber et al., 2005) and its superior capacity to form stable organo-mineral complexes (Eusterhues et al., 2005; Lehmann and Kleber, 2015). Previous studies have demonstrated that organic amendments can enhance the content of non-crystalline Fe oxides, thereby promoting Fe-C associations (Chen et al., 2022; Huang et al., 2017; Wang et al., 2019). Extending these findings, our results provide new mechanistic insight by demonstrating that the increase in non-crystalline Fe oxides is closely linked to manure-induced soil alkalization. Specifically, the significant positive correlation between pH and Fe_o

indicates that the increased pH after manure application (Table 1) created conditions favoring Fe_o preservation (Vithana et al., 2015), with an increase of 25.4% in the content of Fe_o. The higher Fe_o content provided abundant reactive surfaces for MAOM formation. The nature of this interaction likely involves specific molecular-scale binding mechanisms. Recent advances in synchrotron-based spectroscopy (e.g., STXM-NEXAFS) have provided direct evidence that poorly crystalline iron oxides (e.g., ferrihydrite) stabilize organic carbon primarily through ligand exchange, where carboxyl (-COOH) and hydroxyl (-C-OH) functional groups in organic molecules replace the surface hydroxyl groups on Fe oxides (Ruiz et al., 2024). Furthermore, coprecipitation, where organic matter is encapsulated within the matrix of forming Fe (oxyhydr)oxides, represents another potent stabilization mechanism that can generate long-term sinks for organic carbon (Chen et al., 2014). While our bulk data cannot unequivocally distinguish between these mechanisms, the correlation suggests that similar processes are likely operative in our system, contributing to the stability of the large MAOM-C pool. This pH-Fe_o-MAOM nexus establishes a self-reinforcing stabilization mechanism: manure-derived organic ligands interact with Fe_o to form stable complexes, simultaneously protecting both organic carbon and Fe_o from dissolution (Kleber et al., 2021).

The positive correlation between Fe_o and MAOM C (Fig. 3C) suggested that non-crystalline Fe oxides played a critical role in stabilizing SOC through organo-mineral interactions. However, while our data support the association between Fe_o and MAOM C, the underlying mechanisms (e.g., adsorption, co-precipitation, or ligand exchange) remain speculative due to the lack of direct molecular-scale evidence. Future studies employing advanced spectroscopic techniques (e.g., synchrotron-based X-ray absorption spectroscopy or NanoSIMS) could explicitly characterize the binding forms of Fe-organic complexes, thereby validating the causal relationship between Feo and MAOM formation.

4.3. Chemical composition and thermal stability

Input of new organic material could alter chemical composition of SOC and lead to the change of the molecule recalcitrance of SOC (Guo et al.,2019; Yan et al., 2013; Zhou et al., 2010; Zhang et al., 2013). In the current study, pig manure application resulted in a higher proportion of O-alkyl C but a lower proportion of aromatic C. Given pig manure was rich in cellulose and lignin components, its introductionsubstantially increased O-alkyl C relative to the Control (Li et al., 2015). The

considerable accumulation of O-alkyl C accounted for the reduction of the relative proportion of aromatic C and thelower aromaticity.

Long-term pig manure application strengthened SOC thermal stability by improving the content of thermally stable organic matters while it decreased TG-T_{50}. The observed increase in the absolute amount of thermally stable SOC (Exo_2) can be attributed to the formation of stable organo-mineral complexes with newly formed Fe_o. As elucidated by Kleber et al. (2021), the thermal stability of organic matter is significantly enhanced upon binding to mineral surfaces. Thermal analysis suggested that manure amend significantly increased SOM content, evidenced by the increase of the mass losses during 180-530 ℃ (Exo_{tot}) (Table 4). The result was consistent with the change of SOC content measured by conventional method (Table 1), indicating TG technology was promising for measuring SOM content (Siewert, 2004; Tokarski et al., 2018). The decrease of TG-T_{50} reflected more easily decomposable SOC accumulated after manure application (Gao et al., 2015; Siewert, 2004). The result consisted with that in the NMR spectroscopy, where greater O-alkyl C and higher aliphaticity were found under manure treatments (Table 3). SOC with more O-alkyl C functional groups or higher aliphaticity was less likely to resist thermochemical degradation as revealed by the negative relationship between TG-T_{50} and aliphacity (Fig.4; Fig. 5) (Hou et al., 2019; Lehman and Kleber, 2015), thus leading to a decrease of TG-T_{50}. In this study, the thermally labile organic matters accounted for over half of the total organic matters, so the decrease of TG-T_{50} after manure application was just a result of the increased thermally organic matters not the decrease of thermal stability. In contrast, thermal stability should be strengthened according to the increased thermally stable organic matters after manure application. The observed decrease TG-T_{50} and the simultaneous increase in Exo_2 are not contradictory. This apparent paradox can be explained by the dual effect of manure amendment: the input of a large quantity of labile, manure-derived organic compounds significantly increased the proportion of thermally labile C, thereby reducing the average stability of the entire SOM pool (as reflected by the decreased TG-T_{50}). Concurrently, the manure-induced biogeochemical changes (e.g., increased pH and Fe oxide transformation) promoted the formation of highly stable organo-mineral complexes. While the relative proportion of this stable C might be diluted by the new labile C, its absolute amount within the soil system increased substantially, which is captured by the increase in the absolute Exo_2 signal. Since soil structure was destroyed due to the

ground process of soil samples before TG analysis, the increase of the thermally stable organic matters was ascribed to mineral protection, where the correlations between organic carbon and Fe oxides increased the thermally resistance of OC (Ruiz et al., 2023).

5. Conclusion

Manure application increased SOC quantity and improved its quality in Fe-rich red soils. SOC in the POM fraction exhibited the most pronounced response to manure inputs, while the majority of SOC was stored in the MAOM fraction. Furthermore, SOC was stabilized by distinct yet complementary mechanisms: physical protection via aggregation process, and chemical protection via Fe-organic associations induced by elevated pH. In addition, manure application increased thermally stable organic matters. However, to better understand inherent mechanisms, future work should focus on molecular-scale characterization of Fe-organic interactions using synchrotron techniques (e.g., Fe K-edge XANES/EXAFS), and in-situ visualization of POM-mediated aggregation through advanced imaging tools (e.g., SEM-TEM or μ-CT) coupled with ^{13}C-labelled manure to track POM dynamics within aggregates.

Acknowledgments

This work was financially supported by the NSFC-CAS Joint Fund Utilizing Large-scale Scientific Facilities (No. U1832188) and Chinese Universities Scientific Fund (2023RC047). We thank Yanyan Cai and Xing Xia for laboratory assistance.

Author contributions

HR conceived the experimental approach, took soil samples from the field, carried out the laboratory and data analyses, wrote the first draft of the manuscript, and contributed to subsequent drafts. ZLD helped analyze NMR spectrum and revise the manuscript. WDG contributed to interpretating TG data and revising the manuscript. LXM conducted the experiment of NMR. XHP helped design the experiment, and analyze data. YJJ contributed to the design of field experiment and the process of taking soil samples. DMY contributed to the process of writing. HZ contributed to funding acquisition, conceiving the experimental approach, carrying out data interpretations, and the writing of all subsequent manuscript drafts.

Conflict of Interest

Hu Zhou is a member of the editorial board of SOIL.

References

Álvaro-Fuentes, J., Franco-Luesma, S., Lafuente, V., Sen, P., Usón, A., Cantero-Martínez, C., and Arrúe, J.L.: Stover management modifies soil organic carbon dynamics in the short-term under semiarid continuous maize, Soil Till. Res., 213, 105143, https://doi.org/10.1016/j.still.2021.105143, 2021.

Amelung, W., Bossio, D., de Vries, W., Kögel-Knabner, I., Lehmann, J., Amundson, R., Bol, R., Collins, C., Lal, R., Leifeld, J., Minasny, B., Pan, G., Paustian, K., Rumpel, C., Sanderman, J., van Groenigen, J.W., Mooney, S., van Wesemael, B., Wander, M., and Chabbi, A.: Towards a global-scale soil climate mitigation strategy. Nat. Commun., 11, 5427, https://doi.org/10.1038/s41467-020-18887-7, 2020.

Baldock, J.A., Oades, J.M., Nelson, P.N., Skene, T.M., Golchin, A., and Clarke, P.: Assessing the extent of decomposition of natural organic materials using solid-state ^{13}C NMR spectroscopy, Soil Res., 35, 1061–1084, https://doi.org/10.1071/S97004, 1997.

Bai, X.X., Tang, J., Wang, W., Ma, J.M., Shi, J., and Ren, W.: Organic amendment effects on cropland soil organic carbon and its implications: A global synthesis, Catena., 231, 107343, https://doi.org/10.1016/j.catena.2023.107343, 2023.

Benbi, D.K., Boparai, A.K., and Brar, K.: Decomposition of particulate organic matter is more sensitive to temperature than the mineral associated organic matter, Soil Biol. Biochem., 70, 183-192, https://doi.org/10.1016/j.soilbio.2013.12.032, 2014.

Cambardella, C.A., and Elliott, E.J.: Particulate soil organic-matter changes across a grassland cultivation sequenc e, Soil Sci. Soc. Am. J., 5, 777-783, https://doi.org/10.2136/sssaj1992.03615995005600030017x, 1992.

Chen, M., Zhang, S., and Liu, L.: Organic fertilization increased soil organic carbon stability and sequestration by i mproving aggregate stability and iron oxide transformation in saline-alkaline soil. Plant Soil 474, 233–24 9. https://doi.org/10.1007/s11104-022-05326-3, 2022.

Chenu, C., Angers, D.A., Barre, P., Derrien, D., Arrouays, D., and Balesdent, J.: Increasing organic stocks in agricultural soils: Knowledge gaps and potential innovations, Soil Till. Res., 188, 41-52, https://doi.org/10.1016/j.still.2018.04.011, 2019.

Cotrufo, M.F., Ranalli, M.G., Haddix, M.L., Six, J., and Lugato, E.: Soil carbon storage informed by particulate and mineral-associated organic matter, Nature Geosci., 12, 989-996, https://doi.org/10.1038/s41561-019-0484-6, 2019.

Dennis, P.G., Miller, A.J., and Hirsch, P.R.: Are root exudates more important than other sources of rhizodeposits in structuring rhizosphere bacterial communities? FEMS Microbiol Ecol., 72, 313-327, https://doi.org/10.1111/j.1574-6941.2010.00860.x, 2010.

Eusterhues, K., Rumpel, C., and Kögel-Knabner, I.: Organo-mineral association in sandy acid forest soils: importance of specific surface area, iron oxides and micropores, Eur. J Soil Sci., 56, 753-763, https://doi.org/10.1111/j.1365-2389.2005.00710.x, 2005.

Gao, Q.Q., Ma, L.X., Fang, Y.Y., Zhang, A.P., Li, G.C., Wang, J.J., Wu, D., Wu, W.L., and Du, Z.L.: Conservation tillage for 17 years alters the molecular composition of organic matter in soil profile, Sci. Total Environ., 762, 143116, https://doi.org/10.1016/j.scitotenv.2020.143116, 2021.

Gao, W.D., Zhou, T.Z., and Ren, T.S.: Conversion from conventional to no tillage alters thermal stability of orga-n ic matter in soil aggregates, Soil Sci. Soc. Am. J., 79, 585-594, https://doi.org/10.2136/sssaj2014.08.0334. https://doi.org/10.1016/j.scitotenv.2020.143116, 2015.

Garten, C.T., and Wullschleger, S.D.: Soil carbon dynamics beneath switchgrass as indicated by stable isotope analysis, J. Environ. Qual., 29, 645-653. https://doi.org/10.2134/jeq2000.00472425002900020036x, 2000.

Gong, W., Yan, X.Y., Wang, J.Y., Hu, T.X., and Gong, Y.B.: Long-term manure and fertilizer effects on soil organic matter fractions and microbes under a wheat–maize cropping system in northern China, Geoderma, 149, 318-324, https://doi.org/10.1016/j.geoderma.2008.12.010, 2009.

Guo, Z.C., Zhang, J.B, Fan, J., Yang, X.Y., Yi, Y.L., Han, X.R., Wang, D.Z., Zhu, P., and Peng, X.H.: Does animal manure application improve soil aggregation? Insights from nine long-term fertilization experiments. Sci. Total Environ., 660, 1029-1037, https://doi.org/10.1016/j.scitotenv.2019.01.051, 2019.

Hemingway, J.D., Rothman, D.H., Grant, K.E., Rosengard, S.Z., Eglinton, T.I., Derry, L.A., and Galy, V.: Mineral protection regulates long-term preservation of natural organic carbon, Nature, 570, 2717-2726, https://doi.org/10.1038/s41586-019-1280-6, 2019.

Hou, Y.H., Chen, Y., Chen, X., He, K., and Zhu, B.: Changes in soil organic matter stability with depth in two alp-i ne ecosystems on the Tibetan Plateau, Geoderma, 351, 153-162, https://doi.org/10.1016/j.geoderma.2019.05.034, 2019.

Huang, X., Feng, C., and Zhao, G.: Carbon Sequestration Potential Promoted by Oxalate Extractable Iron Oxides t hrough Organic Fertilization. Soil Sci. Soc. Am. J. 81, 1359–1370. https://doi.org/10.2136/sssaj2017.02.0068, 2017.

Jiang, Y.J., Zhou, H., Chen, L.J., Yuan, Y., Fang, H., Luan, L., Chen, Y., Wang, X.Y., Liu, M., Li, H.X., Peng, X.H., and Sun, B.: Nematodes and microorganisms interactively stimulate soil organic carbon turnover in the macroaggregates, Front Microbiol., 9, 2803, https://doi.org/10.3389/fmicb.2018.02803, 2018.

Kleber, M., Bourg, I.C., Coward, E.K., Hamsel, C.M., Myneni, S.C.B., and Nunan. N.: Dynamic interactions at the mineral-organic matter interface, Nat. Rev. Earth Environ., 2, 402–421, https://doi.org/10.1038/s43017-021-00162-y, 2021.

Kleber, M., Mikutta, R., Torn, M.S., and Jahn,R.: Poorly crystalline mineral phases protect organic matter in acid subsoil horizons, Eur. J. Soil Sci., 717-725, https://doi.org/10.1111/j.1365-2389.2005.00706.x, 2005.

Kögel-Knabner, I.: ^{13}C and ^{15}N NMR spectroscopy as a tool in soil organic matter studies, Geoderma, 80, 243-270, https://doi.org/10.1016/S0016-7061(97)00055-4, 1997.

Lal, R.: Soil carbon sequestration impacts on global climate change and food security, Science, 304, 1623-1627, https://doi.org/10.1126/science.1097396, 2004.

Lan, Z.J., Shan, J., Huang, Y., Liu, X. M., Lv, Z.Z., Ji, J.H., Hou, H.Q., Xia, W.J., and Liu, Y.R.: Effects of long-term manure substitution regimes on soil organic carbon composition in a red paddy soil of southern China, Soil Till. Res., 221, 105395, https://doi.org/10.1016/j.still.2022.105395, 2022.

Lavallee, J.M., Soong, J.L., Cotrufo, M.F.: Conceptualizing soil organic matter into particulate and mineral-associated forms to address global change in the 21st century, Glob. Chang Biol., 26, https://doi.org/10.1111/gcb.14859, 2019.

Le, Bissonnais, Y.: Aggregate stability and assessment of soil crustability and erodibility: I. Theory and methodology, Eur. J. Soil Sci., 47,425-437, https://doi.org/10.1111/j.1365-2389.1996.tb01843.x, 1996.

Lehmann, J., Kleber, M.: The contentious nature of soil organic matter, Nature, 528, 60-68, https://doi.org/10.1038/nature16069, 2015.

Li, J., Wen, Y., Li, X., Li, Y., Yang, X., Lin, Z., Song, Z, Cooper, J., and Zhao, B.: Soil labile organic carbon fractions and soil organic carbon stocks as affected by longterm organic and mineral fertilization regimes in the

North China Plain, Soil Till. Res., 175, 281–290, https://doi.org/10.1016/j.still.2017.08.008, 2018.

Li, Z.Q., Zhao, B.Z., Wang, Q., Cao, X.Y., and Zhang, J.B.: Differences in chemical composition of soil organic carbon resulting from long-term fertilization strategies, PLoS One, 10, e0124359, https://doi.org/10.1371/journal.pone.0124359, 2015.

Lian, T.X., Wang, G.H., Yu, Z.H., Li, Y.S., Liu, X.B., and Jin, J.: Carbon input from ^{13}C-labelled soybean residues in particulate organic carbon fractions in a Mollisol. Biol. Fertil. Soils, 52, 331-339, https://doi.org/10.1007/s00374-015-1080-6, 2015.

Liang, C., Schimel, J.P., and Jastrow, J.D.: The importance of anabolism in microbial control over soil carbon storage, Nat. MicrobioL., 2, 1–6, https://doi.org/10.1038/nmicrobiol.2017.105, 2017.

Liu, S. B., Wang, J.Y., Pu, S.Y., Blagodatskaya, E., Kuzyakov, Y., and Razavi, B. S.: Impact of manure on soil biochemical properties: A global synthesis, Sci. Total Environ., 745, 141003, https://doi.org/10.1016/j.scitotenv.2020.141003, 2020.

Mitchell, E., Scheer, C., Rowlings, D., Contrufo, F., Conant, R.T., and Grace, P.: Important constraints on soil organic carbon formation efficiency in subtropical and tropical grasslands, Glob. Change Bio., 27, 5383-5391, https://doi.org/10.1111/gcb.15807, 2021.

Mustafa A., Xu, H., Shah, S.A.A., Abrar, M.M., Maitlo, A.A., Kubar, K.A., Saeed, Q., Kamran, M., Naveed, M., Wang, B.R., Sun N., and Xu, M.G.: Long-term fertilization alters chemical composition and stability of aggregate-associated organic carbon in a Chinese red soil: evidence from aggregate fraction, C mineration, and ^{13}C NMR analyses, J. Soil Sediment, 21, 2483-2496, https://doi.org/10.1007/s11368-021-02944-9, 2021.

Nichitha, C.V, Raghaven, S., Champa, B.V., Ganapathi, G., Sudarshan V., Nandita, S., Ravikumar, D., and Nagaraja, M.S.: Role of organic manures on soil carbon stocks and soil enzyme activities in intensively managemend ginger production systems. Int. J. Recycl. Org. Waste Agric., 1579, https://doi.org/10.30486/IJROWA.2023.1977064.1579, 2023.

Pausch, J., and Kuzyakov, Y.: Carbon input by roots into the soil: Quantification of rhizodeposition from root to ecosystem cell, Global Change Biol., 24, 1-12, https://doi.org/10.1111/gcb.13850, 2018.

Peng, X.Y., Huang, Y., Duan, X.W., Yang, H., and Liu J.X.: Particulate and mineral-associated organic carbon fractions reveal the roles of soil aggregates under different land-use types in a karst faulted basin of China, Catena, 220, 106721, https://doi.org/10.1016/j.catena.2022.106721, 2023.

Poeplau, C., Don, A., Six, J., Kaiser, M., Benbi, D., Chenu, C., Cotrufo, M.F., Derrien, D., Gioacchini, P., Grand, S., Gregorich, E., Griepentrog, M., Gunina, A., Haddix, M., Kuzyakov, Y., Kühnel, A., Macdonald, L.M., Soong, J., Trigalet, S., Vermeire, M.-L., Rovira, P., van Wesemael, B., Wiesmeier, M., Yeasmin, S., Yevdokimov, I., and Nieder, R.: Isolating organic carbon fractions with varying turnover rates in temperate agricultural soils – A comprehensive method comparison, Soil Biol. Biochem., 125, 10-26, https://doi.org/10.1016/j.soilbio.2018.06.025, 2018.

Ruiz, F., Rumpel, C., Dignac, M-F., Baudin, F., and Ferreira, T. O.: Combing thermal analyses and wet-chemical extractions to assess the stability of mixed-nature soil orgnaic matter, Soil Biol. Biochem., 187, 109216, https://doi.org/10.1016/j.soilbio.2023.109216, 2023.

Ruiz, F., Bernardino, A. F., Queiroz, H. M., Otero, X. L., Rumpel, C., and Ferreira, T. O.: Iron's role in soil organic carbon (de)stabilization in mangroves under land use change, Nat. Commun., 10433, https://doi.org/10.1038/s41467-024-54447-z, 2024.

Shi, R.Y., Liu, Z.D., Li, Y., Jiang, T.M., Xu, M.G., Li, J.Y., and Xu, R.K.: Mechanisms for increasing soil resistance to acidification by long-term manure application, Soil Till. Res., 185, 77-84, https://doi.org/10.1016/j.still.2018.09.004, 2019.

595 Siewert, C.: Rapid screening of soil properties using thermogravimetry, Soil Sci. Soc. Am. J. 68, 1656-1661,
596 https://doi.org/10.2136/sssaj2004.1656, 2004.
597 Simpson, M.J., and Simpson, A.J.: The chemical ecology of soil organic matter molecular constituents, J. Chem.
598 Ecol., 38, 768–784, https://doi.org/10.1007/s10886-012-0122-x, 2012.
599 Six, J., Elliot, E.T., and Paustian, K.: Soil macroaggregate turnover and microaggregate formation: a mechanism for
600 C sequestratioin under no-tillage agriculture, Soil Biol. Biochem., 32, 2099-2103,
601 https://doi.org/10.1016/S0038-0717(00)00179-6, 2000.
602 Six, J., Conant, R.T., Paul, E.A., and Paustian, K.: Stabilization mechanisms of soil organic matter: Implications for
603 C-saturated of soils, Plant Soil, 241, 155-176, https://doi.org/10.1023/A:1016125726789, 2002.
604 Soil Survey Staff.: Soil survey laboratory information manual. Soil survey investigations report No. 45, version 2.0.
605 R. Burt (ed.). U.S. Department of Agriculture, Natural Resources Conservation Service.
606 https://www.nrcs.usda.gov/sites/default/files/2022-10/SSIR45.pdf, 2011.
607 Song, X.X., Wang, P., van Z, L., Bolan, N., Wang, H.L., Li, X.M., Cheng, K., Yang, Y., Wang, M., Liu, T.X., and Li,
608 F.B.: Towards a better understanding of the role of Fe cycling in soil for carbon stabilization and
609 degradation, Carbon Research, 1, 5, https://doi.org/10.1007/s44246-022-00008-2, 2022.
610 Tokarski, D., Kučerík, J., Kalbitz, K., Demyan, M.S., Merbach, I., Barkusky, D., Ruehlmann, J., and Siewert, C.:
611 Contribution of organic amendments to soil organic matter detected by thermogravimetry, J. Plant Nutr.
612 Soil Sci., 181, 664-674, https://doi.org/10.1002/jpln.201700537, 2018.
613 Vithana, C.L., Sullivan, L.A., Burton, E.D., and Bush, R.T.: Stability of schwertmannite and jarosite in an acidic la
614 ndscape: Prolonged field incubation, Geoderma, 239-240, 47-57, https://doi.org/10.1016/j.geoderma.201
615 4.09.022, 2015.
616 Volkov, D.S., Rogova, O.B., Proskurnin, M.A., Farkhodov, Y.R., and Markeeva, L.B.: Thermal stability of organic
617 matter of typical chernozems under different land uses, Soil Till. Res., 197, 104500,
618 https://doi.org/10.1016/j.still.2019.104500, 2020.
619 Wang, S.B., Hu, K.L., Feng, P.Y., Wei, Q., and Leghari, S.J.: Determining the effects of organic manure substitution
620 on soil pH in Chinese vegetable fields: a meta-analysis, J. Soil. Sediment, 23, 118-130,
621 https://doi.org/10.1007/s11368-022-03330-9, 2023.
622 Wang, P., Wang, J., and Zhang, H.: The role of iron oxides in the preservation of soil organic matter under long-term
623 fertilization. J. Soils Sediments 19, 588–598. https://doi.org/10.1007/s11368-018-2085-1, 2019.
624 Wu, J.J., Zhang, H., Pan, Y.T., Cheng, X.L., Zhang, K.R., and Liu G.H.: Particulate organic carbon is more sensitive
625 to nitrogen addition than mineral-associated organic carbon: A meta-analysis, Soil Till. Res., 232, 105770,
626 https://doi.org/10.1016/j.still.2023.105770, 2023.
627 Yan, X., Zhou, H., Zhu, Q.H., Wang, X.F., Zhang, Y.Z., Yu, X.C., and Peng, X.H.: Carbon sequestration efficiency
628 in paddy soil and upland soil under long-term fertilization in southern China, Soil Till. Res., 130, 42-51,
629 https://doi.org/10.1016/j.still.2013.01.013, 2013.
630 Zhang, J.C., Zhang, L., Wang, P., Huang, Q.W., Yu, G.H., Li, D.C., Shen, Q.R., and Ran, W.: The role of non-
631 crystalline Fe in the increase of SOC after long-term organic manure application to the red soil of southern
632 China, Eur. J. Soil Sci. 64, 797-804, https://doi.org/10.1111/ejss.12104, 2013.
633 Zhang, B.Y., Dou, S., Guo, D., and Guan, S.: Straw inputs improve soil hydrophobicity and enhance organic carbon
634 mineralization, Agronomy, 13, 2618, https://doi.org/10.3390/agronomy13102618, 2023.
635 Zhou, P., Pan, G.X., Spaccini, R., and Piccolo, A.: Molecular changes in particulate organic matter (POM) in a typical
636 Chinese paddy soil under different long-term fertilizer treatments, Eur. J. Soil Sci., 61, 231-242,
637 https://doi.org/10.1111/j.1365-2389.2009.01223.x, 2010.
638 Zhou, H., Fang H., Zhang, Q., Wang, Q., Chen, C., Mooney, S. J., Peng X.H., and Du, Z. L.: Biochar enhances soil

hydraulic function but not soil aggregation in a sandy loam, Eur. J. Soil Sci., 70, 291-300, https://doi.org/10.1111/ejss.12732, 2019.

Zou, Z.C., Ma, L.X., Wang, X., Chen, R.R., Jones, D.L., Bol, R., Wu, D., and Du, Z.L.: Decadal application of mineral fertilizers alters the molecular composition and origins of organic matter in particulate and mineral-associated fractions, Soil Biol. Biochem., 182, 109042, https://doi.org/10.1016/j.soilbio.2023.109042, 2023.

Table 1

Soil organic carbon (SOC), total nitrogen (TN), the ration of SOC to TN (SOC/TN), pH, crystalline iron oxides (Fe_d), non-crystalline iron oxides (Fe_o), aggregate size distribution and mean weight diameter (MWD) of water-stable aggregates under no manure (Control), low manure (LM), high manure (HM) and high manure plus lime (HML) treatments.

Treatments	SOC (g kg^{-1})	TN (g kg^{-1})	SOC/TN	pH	Fe_d (g kg^{-1})	Fe_o (g kg^{-1})	Aggregate size distribution (g g^{-1})			MWD (mm)
							>0.25 mm	0.05-0.25 mm	<0.05 mm	
Control	4.79c	0.67c	7.10b	4.80c	62.99a	1.81b	0.67c	0.28a	0.05a	0.98b
LM	7.91b	1.00b	7.94a	5.42c	59.98a	1.74b	0.71b	0.25a	0.04ab	1.09b
HM	10.37a	1.35a	7.69ab	6.11b	59.59a	2.25a	0.77a	0.19b	0.03b	1.22a
HML	10.86a	1.40a	7.76ab	7.08a	62.22a	2.29a	0.78a	0.18b	0.04ab	1.32a

Values are the means (n=3). Different lowercase letters after values in the same row indicate a significant difference among four manure treatments ($P < 0.05$). Fed: crystalline oxides; Feo: non crystalline oxides.

Table 2

Mass proportion, SOC concentration and contribution of the mineral-associated organic matter (MAOM) (<53 μm) fraction, particulate organic matter (POM) (>53 μm) fraction under no manure (Control), low manure (LM), high manure (HM) and high manure plus lime (HML) treatments.

Treatments	Mass proportion (%)		SOC concentration (g C kg^{-1} soil)		Contribution to total SOC/%	
	MAOM	POM	MAOM	POM	MAOM	POM
Control	74.3a	16.6b	4.18c	0.44c	82.4a	8.8c
LM	75.1a	17.2ab	5.61b	1.26b	71.0b	15.9b
HM	73.9a	19.4a	6.81a	2.46a	65.8b	23.7a
HML	72.5a	19.3a	7.09a	2.84a	65.4b	26.0a

Values are the means (n=3). Different lowercase letters after values in the same row indicate a significant difference among four manure treatments ($P < 0.05$). Calculations follow the methodology described in Section 2.4.

Table 3

The contents of various C functional groups in CPMAS-^{13}C-NMR spectra under no manure (Control), low manure (LM), high manure (HM) and high manure plus lime (HML) treatments. Alkyl (0-45 ppm); O-alkyl C (45-110 ppm); aromatic C (110-160 ppm) and carbonyl C (160-220 ppm).

Treatments	alkyl C (%)	O-alkyl C (%)	aromatic C (%)	carbonyl C (%)	alkyl C/ O-alkyl C	aromaticity (%)	aromatic C/O-alkyl C	aliphatic C/ aromatic C	aliphaticity (%)
Control	25.4b	44.9c	15.3a	14.4a	0.57a	17.9a	0.34a	4.58b	82.1b
LM	26.2ab	47.4a	13.3b	13.1b	0.55b	15.3b	0.28b	5.53a	84.7a
HM	26.6a	46.1b	13.4b	13.9ab	0.58a	15.6b	0.29b	5.41a	84.4a
HML	26.5a	45.9b	13.3b	14.3a	0.58a	15.6b	0.29b	5.43a	84.4a

Values are the means (n=3). Different lowercase letters after values in the same row indicate a significant difference among four manure treatments ($P < 0.05$). Aromaticity = aromatic C/ (alkyl C + O-alkyl C + aromatic C); aliphatic C = (alkyl C + O-alkyl C); aliphaticity = (alkyl C + O-alkyl C) / (alkyl C + O-alkyl C + aromatic C).

Table 4

The mass losses during specific temperature ranges under no manure (Control), low manure (LM), high manure (HM) and high manure plus lime (HML) treatments. Exo_1 represents thermally labile soil organic matter (SOM); Exo_2 represents thermally stable SOM; Exo_{tot} represents total SOM. TG-T_{50} indicates the temperature at which half of the total SOM is lost.

Treatments	Exo_1 (180~380℃) (%)	Exo_2 (380~530℃) (%)	Exo_{tot} (180~530℃) (%)	Exo_1/Exo_{tot}	TG-T_{50} (℃)
Control	2.28c	2.36b	4.64b	0.49b	381a
LM	2.62b	2.54a	5.16a	0.51a	376ab
HM	2.69ab	2.68a	5.37a	0.50b	369b
HML	2.89a	2.56a	5.45a	0.53a	371b

Values are the means (n=3). Different lowercase letters after values in the same row indicate a significant difference among four manure treatments ($P < 0.05$).

Figure legends

687 **Fig. 1** CPMAS-^{13}C-NMR spectra under no manure (Control), low manure (LM), high manure (HM) and high
688 manure plus lime (HML) treatments. Alkyl (0-45 ppm); O-alkyl C (45-110 ppm); aromatic C (110-160 ppm) and
689 carbonyl C (160-220 ppm)
690
691 **Fig. 2** Thermogravimetry (TG) curves (a) and corresponding derivative thermogravimetry (DTG) curves (b) of soil
692 organic matter (SOM) under no manure (Control), low manure (LM), high manure (HM) and high manure plus
693 lime (HML) treatments
694
695 **Fig. 3** The relationships between SOC and variables related to the chemical protection and physical protection
696
697 **Fig. 4** Relationship between soil pH and iron oxides concentrations.
698
699 **Fig. 5** Biplots of the principal component analysis (PCA) between the quantity and quality of SOC and variables
700 related to chemical protection, physical protection across four manure application treatments (CK, Control; LM,
701 low manure; HM, high manure; and HML, high manure plus lime)
702
703 **Fig. 6** The relationships between SOC quantity, chemical recalcitrance and thermal stability

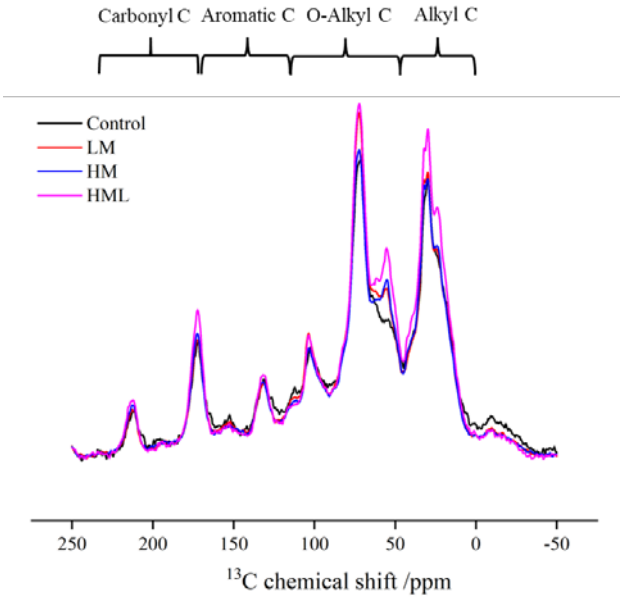

Fig.1 CPMAS-^{13}C-NMR spectra under no manure (Control), low manure (LM), high manure (HM) and high manure plus lime (HML) treatments. Alkyl (0-45 ppm); O-alkyl C (45-110 ppm); aromatic C (110-160 ppm) and carbonyl C (160-220 ppm). The spectra are normalized to the total integral area of the control spectrum to highlight differences in the relative abundances of carbon functional groups.

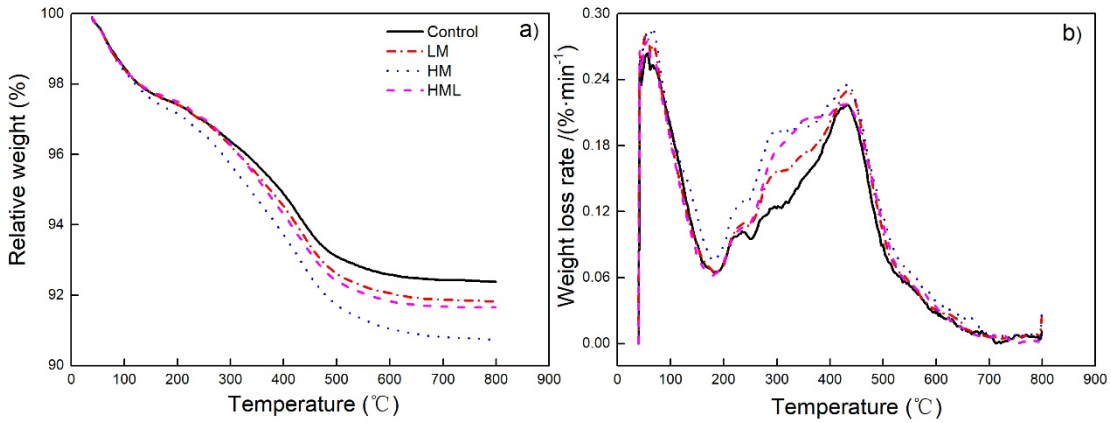

Fig. 2 Thermogravimetry (TG) curves (a) and corresponding derivative thermogravimetry (DTG) curves (b) of soil organic matter (SOM) under no manure (Control), low manure (LM), high manure (HM) and high manure plus lime (HML) treatments

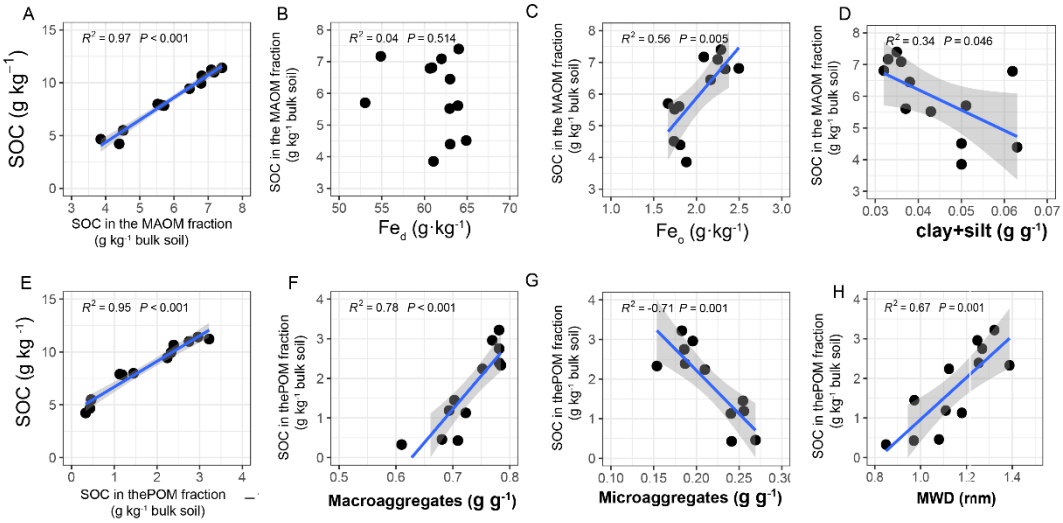

Fig. 3 The relationships between SOC and variables related to the chemical protection and physical protection. (A to D) Variables characterizing chemical protection, including the content of SOC stored in the MAOM fraction, the content of crystalline Fe oxides (Fe_d), the content of non-crystalline Fe oxides (Fe_o), and the content of clay and silt. (E to H) Variables characterizing physical protection, including the content of SOC stored in the POM fractions, the content of soil macroaggregates, the content of soil microaggregates and the mean weight diameter (MWD)

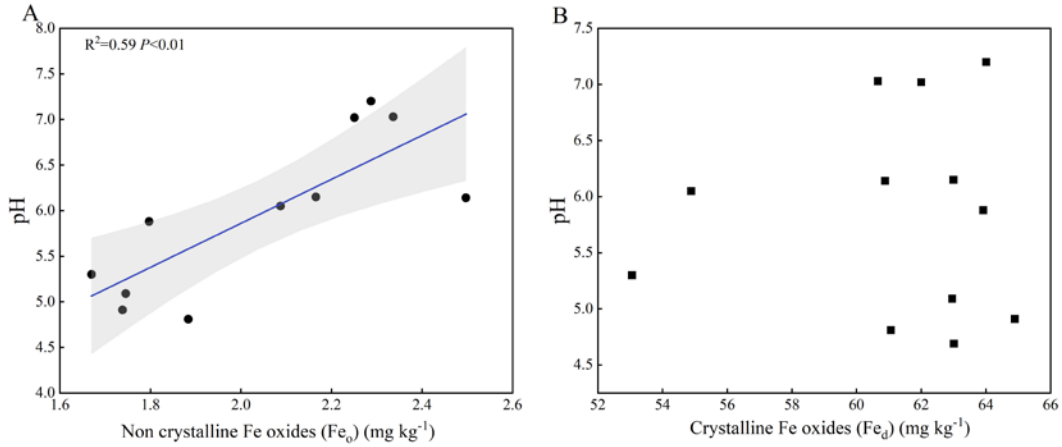

Fig. 4 Relationship between soil pH and iron oxides concentrations. (A) Significant positive correlation between pH and amorphous iron oxides (Fe_o). (B) No significant correlation between pH and crystalline iron oxides (Fe_d).

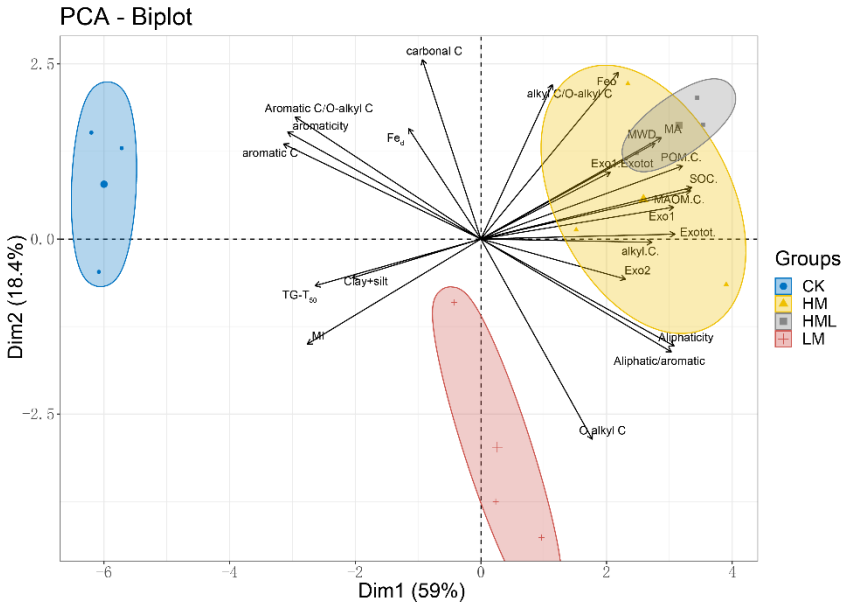

Fig. 5 Biplots of the principal component analysis (PCA) between the quantity and quality of SOC and variables related to chemical protection, physical protection across four manure application treatments (CK, Control; LM, low manure; HM, high manure; and HML, high manure plus lime). Fe_d, crystalline Fe oxides; Fe_o, non-crystalline Fe oxides; MA, macroaggregates (>0.25 mm); MI, microaggregates (0.05-0.25 mm); MWD, mean weight diameter; aromaticity, aromatic C / (alkyl C + O-alkyl C + aromatic C); aliphatic C, Alkyl C + O-alkyl C; aliphaticity, (Alkyl C + O-alkyl C) / (Alkyl C + O-alkyl C + Aromatic C); Exo_1, thermally labile soil organic matter (SOM); Exo_2, thermally stable SOM; Exo_{tot}, total SOM; TG-T_{50}, the temperature at which half of the total SOM was lost

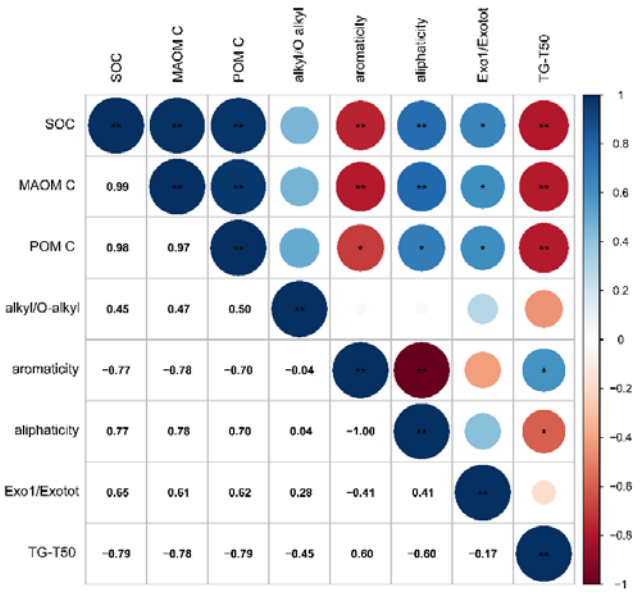

Fig. 6 The relationships between SOC quantity, chemical recalcitrance and thermal stability. Aromaticity, aromatic C / (alkyl C + O-alkyl C + aromatic C); aliphaticity, (alkyl C + O-alkyl C) / (alkyl C + O-alkyl C + aromatic C); Exo_1, thermally labile soil organic matter (SOM); Exo_{tot}, total SOM; TG-T_{50}, the temperature at which half of the total SOM was lost